

## MINERALOGICAL COMPOSITION, ISOTOPIC AND GEOCHEMICAL CHARACTERISTICS OF PLEISTOCENE GLENDONITES FROM THE OUTCROPS OF BOL'SHAYA BALAKHNYA RIVER, EASTERN TAIMYR, RUSSIA

KSENIYA VASILEVA,<sup>1</sup> VICTORIA ERSHOVA,<sup>1,2</sup> MIKHAIL ROGOV,<sup>2</sup> JULIA GRITSENKO,<sup>3,4</sup> FEDOR MAXIMOV,<sup>1</sup> YAROSLAV OVSEPYAN,<sup>2</sup>

TATIANA OKUNEVA,<sup>5</sup> ANNA RYBAKOVA,<sup>5</sup> DARIA KISELEVA,<sup>5</sup> AND OLEG VERESHCHAGIN<sup>1</sup>

<sup>1</sup>St. Petersburg State University, Institute of Earth Sciences, University Embankment 7/9, 199034 St. Petersburg, Russia

<sup>2</sup>Geological Institute of RAS, Pyzhevski Lane 7, 119017 Moscow, Russia

<sup>3</sup>Faculty of Geology, GSP-1, 1 Leninskiye Gory, 119991 Moscow, Russia

<sup>4</sup>Fersman Mineralogical Museum, Leninskiy Prospect 18–2, 119071 Moscow, Russia

<sup>5</sup>Zavaritsky Institute of Geology and Geochemistry, Ural Branch of Russian Academy of Science, 620016 Ekaterinburg, 15 Akademika Vonsovskogo Street, Russia

e-mail: k.vasilyeva@spbu.ru

**ABSTRACT:** We present a complex study on mineralogical, U/Th dating, isotopic and geochemical characteristics of Pleistocene glendonites (calcite pseudomorphs after ikaite) from the outcrops of Bol'shaya Bakakhnya valley, eastern Taimyr, Russia. Based on the U/Th dating of the glendonites ( $37 \pm 7$  ka) we propose that the glendonites and host sediments were formed during the Karginsky interstadial (22–50 ka)—this data corresponds well with published ages of foraminifers and wood fragments from Karginsky deposits of eastern Taimyr. The main factors leading to ikaite crystallization was presence of organic matter ( $\delta^{13}\text{C}$  varies from  $-5$  to  $-40\%$  V-PDB) in the host clayey sediments and low temperatures ( $< 7^\circ\text{C}$ ) of bottom water. Isotope ( $\delta^{18}\text{O}$  ratios vary from  $-8$  to  $-33.9\%$  V-PDB) and geochemical (PAAS-normalized patterns of rare earth elements) characteristics of the studied glendonites confirm that ikaite crystallization and transformation was influenced by seawater. Carbon was derived from dissolved inorganic carbon, decomposed organic matter, and probably methane. Some glendonites are surrounded by concretions (host rock cemented by calcite). The isotopic characteristics of the host concretions and glendonites are similar, so we assume that glendonites and host nodules were formed by the same processes—sulfate reduction coupled with anaerobic decomposition of organic matter. Nevertheless, geochemical characteristics of the host concretions and glendonites differ: Mg/Ca ratio and values of Fe, Mn, Zn, Cd, and U are higher in host concretion than in glendonite. This may reflect differences in crystalline structure of ikaite and high magnesium calcite.

### INTRODUCTION

Glendonites are pseudomorphs after ikaite—metastable hexahydrate of calcium carbonate ( $\text{CaCO}_3 \cdot 6\text{H}_2\text{O}$ ) found all over the world in a wide range of depositional settings and stratigraphical intervals (see Rogov et al. 2021, 2023 and references therein). In modern environments, ikaite is stable under near-freezing conditions (Whiticar and Suess 1998; Greinert and Derkachev 2004; Krylov et al. 2015). Ikaite precipitates during early diagenesis promoted by an alkaline geochemical environment and  $\text{CO}_2$  release due to reactions of sulfate reduction (Qu et al. 2017; Whiticar et al. 2022). Glendonite forms due to ikaite dehydration and cementation under increasing temperatures.

Based on finds of modern ikaite in low-temperature environments, glendonites are often considered by researchers as indicators of cold-water environments of the past (Frank et al. 2008; Vickers et al. 2018, 2022, 2023 among others). Nevertheless, sometimes based on low ratios of  $\delta^{13}\text{C}$  values, methane seeps are thought to influence ikaite precipitation (Teichert and Luppold 2013; Morales et al. 2017).

Stratigraphic studies and various dating techniques for Quaternary deposits provide data for high-resolution stratigraphy, which makes possible the precise correlation of glendonite findings and climatic changes. Furthermore, the

study of Quaternary glendonites less affected by later diagenetic alteration, and thus better preserved than ancient ones, could provide additional information about the environment of ikaite crystallization and its transformation into glendonite. However, only a few studies on Quaternary glendonites from the White Sea (Schultz et al. 2022; Vasileva et al. 2022) and Alaska (Jacobson 2014; Schultz et al. 2022) have yet been published.

Glendonites from outcrops of the Bol'shaya Balakhnya River valley in northern Taimyr were briefly described in the 1980s (Brodskaya and Rengarten 1975), and later have been mentioned in several publications (Kind and Leonov 1982; Mokhov and Proskurnin 2015; Delventhal 2022). The purpose of this study is to determine mineralogical, isotopic and geochemical characteristics of glendonites from outcrops of the Bol'shaya Balakhnya River valley and reconstruct the processes of ikaite precipitation and transformation into glendonite.

### GEOLOGICAL FRAMEWORK AND THE STUDIED SECTION

Glendonites are described from two sections located in the eastern part of the Taimyr Peninsula. Their frequent occurrences in the Aragonitovoye and Snezhnoe sites (Figs. 1, 2), located on the banks of the river Bol'shaya

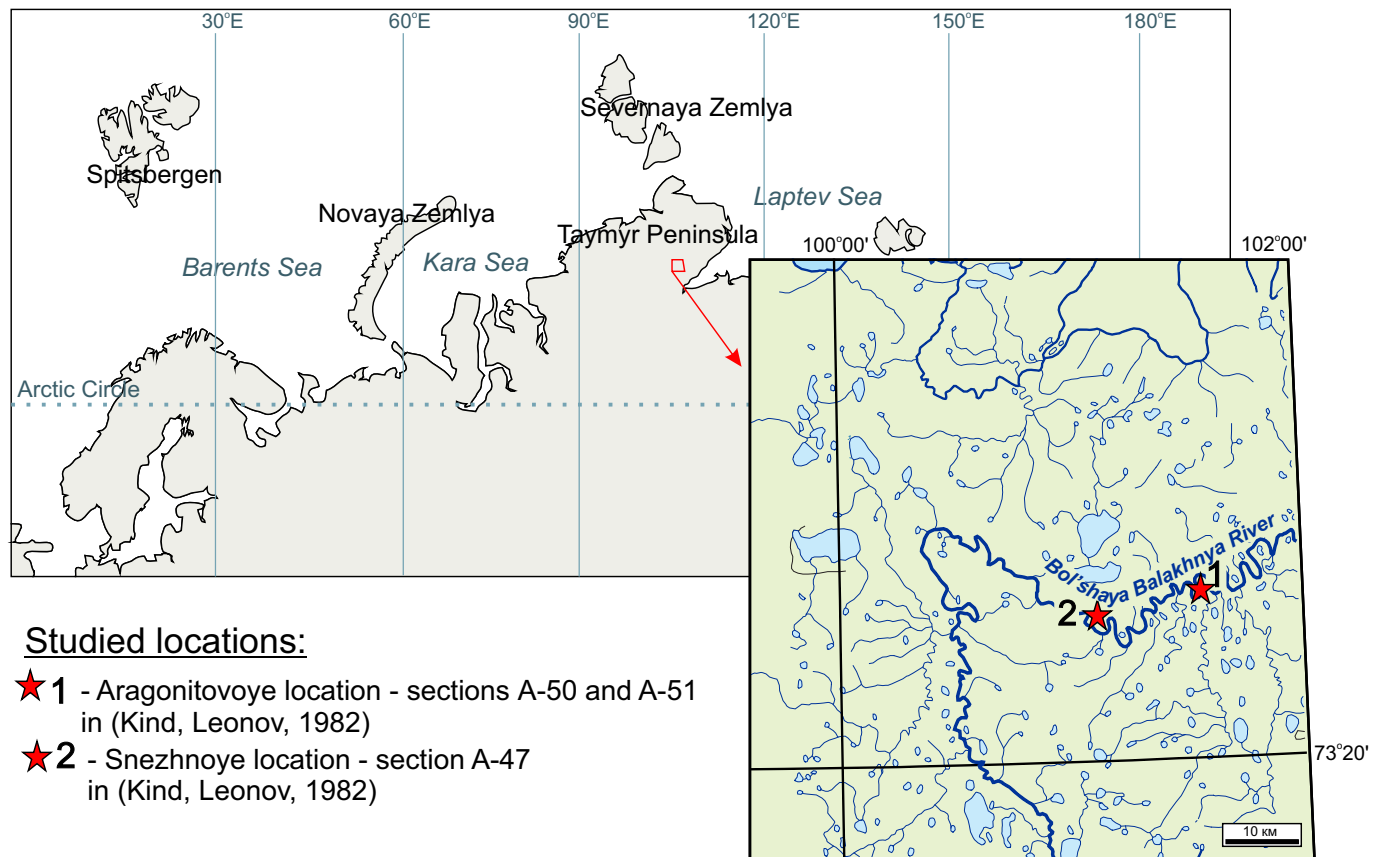


FIG. 1.—Studied localities and their geographical position.

Balakhnya, were discovered by S.M. Andreeva and L.V. Lopatina in 1973 during a geological survey (Fisher et al. 1989). The Aragonitovoye section (the overall thickness is 3–6 meters) is composed of sands with lenses of clay (10–40 cm thick), the glendonites are found within clay. The Snezhnoye site is located on the bank of the Bol'shaya Balakhnya River, near Deptumalaturku Lake (Fig. 1). The section here is composed of sands with clay lenses (30–60 cm thick); the glendonites are found in clays. Soon after discovery of these glendonites a few specimens (referred as recorded from Bol'shaya Balakhnya without additional data) were briefly described by Brodskaya and Rengarten (1975). These authors note the presence of glendonites in clayey host rock (with suggested age 30–40 ka). Numerous well-preserved glendonites from one of these localities were collected in the late 1970s by L.D. Sulzerzhitsky (Geological Institute, Moscow), who donated them to the Vernadsky State Geological Museum in Moscow; some of these specimens were referenced recently by Rogov et al. (2021, their Fig. 1.5; 2023, their Figs. 2.3, 14.7–9). However, details about the locality (or localities) as well as precise geological information concerning these specimens was missing: only their origin from the Quaternary deposits of the Bol'shaya Balakhnya River was clear.

The age of the host rocks is determined differently. Mokhov and Proskurnin (2015) propose that the host sediments correspond to the Kazantsevo Formation (marine sediments deposited during the Kazantsevo interglacial), while Kind and Leonov (1982) assign the host sediments to the Karginy interstadial (see Discussion).

#### MATERIALS AND METHODS

Five samples of glendonites from the Aragonitovoye locality and one sample from the Snezhnoye locality (Table 1) were derived from the dark-colored Quaternary clays by one of the authors (JG) during the fieldwork in the

summer of 2018. Along with glendonites one sample of host clay was examined for microfossil analysis.

Glendonite samples were studied to find out their mineralogy, geochemical, isotopic composition and age. The mineral composition was studied using the powder X-ray diffraction (PXRD) technique on a Rigaku Miniflex II diffractometer (CuK $\alpha$  radiation, 5–80°, 3°/min scan speed). Petrographic and cathodoluminescence (CL) studies were carried out on polished thin sections on an Olympus BX-53 microscope with a CL8200 Mk5–2 Optical CL system. For evaluating geochemical composition, we used a Perkin Elmer ICP-AES Optima 8000 DV (Ca, Mg, Fe) and ICP-MS NexION 300S (Perkin Elmer) (REE, Sr, Rb, Cu, Ni, Mn, Zn, Cd, U). Powdered samples weighing 0.1–1.5 g were leached for 30 minutes in 0.01 M HCl. Once the samples were separated from the insoluble residue in the centrifuge, they were leached in 2.5 ml 0.1 N HCl and 3.5 ml 1 M HCl. The samples were then evaporated and leached in 3% HNO<sub>3</sub>, with chemical analyses made on 50 ml of solution. The obtained concentrations of major and trace elements in the standard material are in satisfactory agreement with certified values, with a deviation of < 15%. The  $\delta^{13}\text{C}$  and  $\delta^{18}\text{O}$  isotope ratios were measured using the Thermo electron system, including a Delta V Advantage Mass Spectrometer with Gas-Bench-II. Analytical precision for both  $\delta^{18}\text{O}$  and  $\delta^{13}\text{C}$  was  $\pm 0.2$ . The results of measurements of isotope compositions of stable carbon and oxygen isotopes presented as  $\delta^{13}\text{C}$  (‰ V-PDB, Vienna PeeDee Belemnite) and  $\delta^{18}\text{O}$  (‰ V-PDB). We used the  $^{230}\text{Th}/\text{U}$  dating method to determine the ages of the glendonites. Four subsamples of the glendonites (sample Bal-4) were radiochemically analyzed using the “total sample dissolution” (TSD) technique (Bischoff and Fitzpatrick 1991; Maksimov and Kuznetsov 2010). To exclude the influence of contamination with  $^{232}\text{Th}$  from clastic components, isochrons were plotted (Bischoff and Fitzpatrick 1991; Rowe and Maher 2000; Geyh 2008). Radiometric measurements of U and Th isotopes was carried out on an



FIG. 2.—Photographs of Aragonitovoye locality with numerous loose glendonite specimens.

OR-TEC's Alpha Suite Alpha Spectrometer. Normalization of the analytical isotopic data against  $^{232}\text{Th}$  allowed us to build linear isochrons using  $^{230}\text{Th}/^{232}\text{Th}$ – $^{234}\text{U}/^{232}\text{Th}$  and  $^{234}\text{U}/^{232}\text{Th}$ – $^{238}\text{U}/^{232}\text{Th}$  coordinates, as well as to calculate the  $^{230}\text{Th}/^{234}\text{U}$  and  $^{234}\text{U}/^{238}\text{U}$  activity ratios and age of the carbonate fraction, based on methods given in Geyh (2008) and Maksimov and Kuznetsov (2010).

Microfauna were analyzed in the fraction  $> 63 \mu\text{m}$ , and the species composition of fossil foraminifers and ostracods was studied under the binocular microscope. Photos were taken with a VEGA3 TESCAN scanning

electron microscope (SEM) at the Borissiak Paleontological Institute, Russian Academy of Sciences, and on the light microscope ADF W300, with digital camera STD16 at the Geological Institute, Russian Academy of Sciences.

## RESULTS

### *Morphology of the Studied Glendonites*

The studied glendonites predominantly comprise rosette forms that reach 4.5 cm in diameter (Fig. 3); samples Bal-4 and Sn-1 represent two glendonites enclosed by a concretion; sample Bal-3 is represented by three glendonites, gravel particles, and wood fragments enclosed by a carbonate concretion. The sample Bal-1 has an elongated form and encloses a wood fragment. Sample Bal-6 has a bladed form. Sample Bal-2 is a single glendonite in a carbonate concretion.

### *Taxonomic Identification of Microfossils*

Qualitative analysis of the clay sample show the presence of benthic foraminifera tests and ostracod valves belonging to the typical Arctic fauna (Pleistocene–Modern) of shallow shelf areas influenced by river runoff. Benthic foraminifera are represented by the species *Buccella frigida* (Cushman 1922), *Elphidium clavatum* (Cushman 1930), *Elphidium albiumbilicatum* (Weiss 1954), *Eoepionidella pulchella* (Parker 1952), and *Haynesina orbiculare* (Brady 1881) (Fig. 4). Ostracods valves are rare and belong to three species: *Roundstonia macchesneyi* (Brady and Crosskey

TABLE 1.—Mineralogy of the studied samples (data obtained by powder X-ray diffraction).

No.	Sample	Calcite	Dolomite	Quartz	Plagioclase
1	Bal-1 (glendonite)	■			
2	Bal-1 (host concretion)	■		±	
3	Bal-2 (glendonite)	■			
4	Bal-2 (concretion)	■	±	□	±
5	Bal-3 (glendonite)	■			
6	Bal-4 (glendonite)	■		±	
7	Bal-4 (host concretion)	■			
8	Bal-5 (glendonite)	■		□	±
9	Bal-6 (glendonite)	■		±	
10	Sn-1 (glendonite)	■		±	

Note: ■, main phase; □, minor phase; ±, traces.

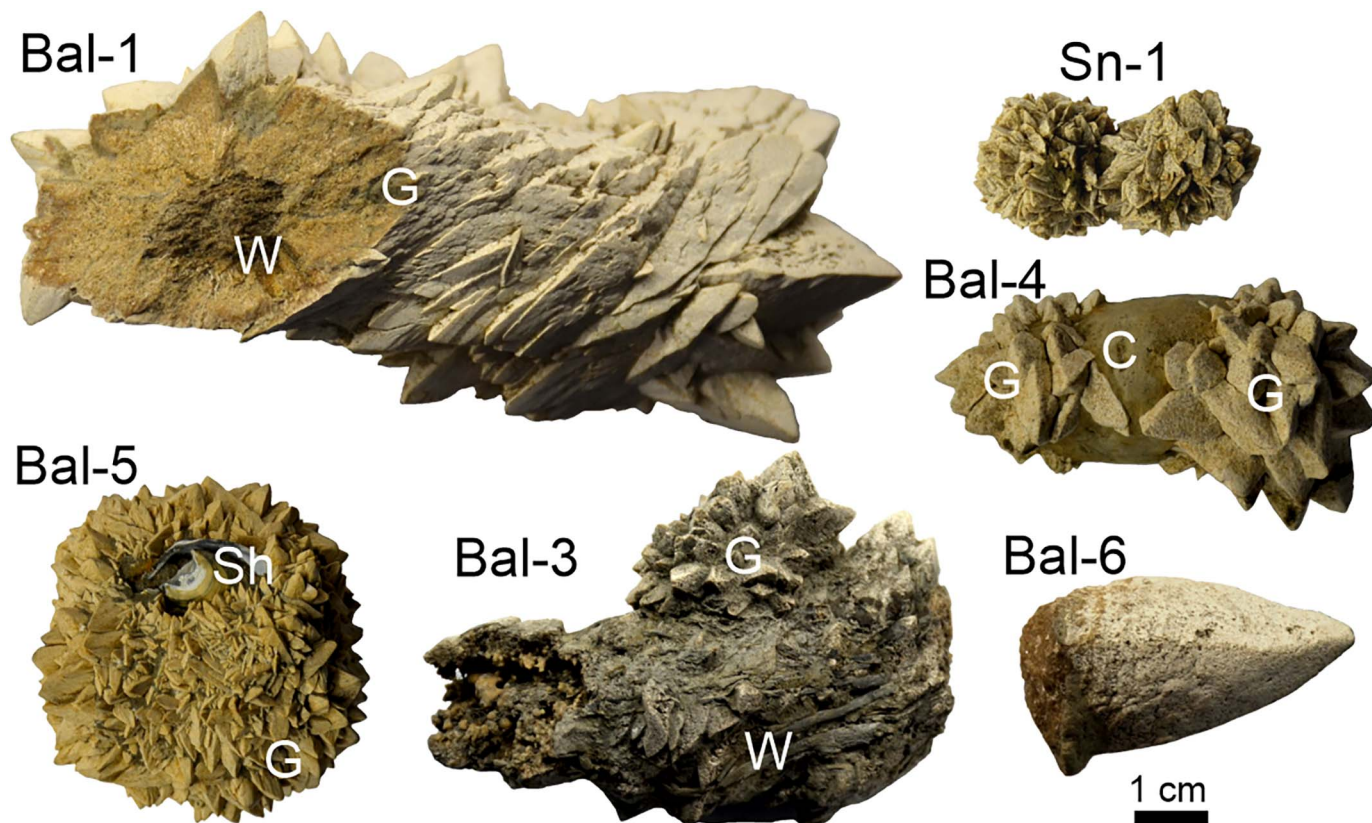


FIG. 3.—Morphology of the studied glendonites. W, wood fragment; G, glendonite; C, carbonate concretion; Sh, bivalve shell fragment.

1871), *Semicytherura complanata* (Brady et al. 1874), and *Sarsicytheridea bradii* (Norman 1864) (Fig. 4). The preservation of microfossils is rather good, but foraminifera tests are found mostly in the fine fraction, 63–125  $\mu\text{m}$ .

#### Mineralogical Composition and Optical Studies

PXRD data show that the studied glendonites and concretions are composed of calcite with minor amounts of dolomite, quartz, and feldspar (Table 1). Optical studies reveal that glendonites are composed of slightly elongated oval or tabular crystals and rosette-like joints of elongated crystals of calcite. The size of calcite crystals is up to 0.4 mm. Calcite crystals are zonal: the central zone is dark (almost black, see Fig. 5A–C; central zones of the calcite crystals are shown with white arrows); a thin brown rim appears around the edges. Outside, the crystals are surrounded by a thin colorless zone. Carbonate minerals are non-luminescent in CL.

The host concretions (samples Bal-1, Bal-2, Bal-4) are composed of micrite with minor amounts of clastic silty grains of quartz and feldspar (Fig. 5D); clastic grains show blue and red luminescence, while carbonate minerals are non-luminescent.

#### Isotope Analyses

Isotope studies (Table 2, Fig. 6) reveal that both glendonites and host concretions show a wide range of isotope values.  $\delta^{13}\text{C}$  values in glendonites vary from  $-33.9$  to  $-6.2\text{‰}$  V-PDB (mean value  $-18.2\text{‰}$  V-PDB), while  $\delta^{18}\text{O}$  values vary from  $-3.5$  to  $-1.1\text{‰}$  V-PDB. In host concretions both oxygen and carbon isotope values vary slightly from the enclosed glendonite.  $\delta^{13}\text{C}$  values in concretions vary from  $-22.3$  to  $-6.7\text{‰}$  V-PDB and  $\delta^{18}\text{O}$  values vary from  $-4.2$  to  $-2.9\text{‰}$  V-PDB.

#### Geochemical Characteristics

The geochemical composition of the studied glendonites and host concretions are given in the Supplemental Table 1S and Figures 7, 8, and 9. Concretions are characterized by elevated values of some elements compared to glendonites. The concentration of Fe in glendonites is 0.01–0.04%, while in concretions it rises to 0.99 and 1.55%; concentration of Zn in glendonite varies from 0.8 to 1.4 ppm, in concretions content of Zn is 15–16 ppm; Mn concentrations in concretions are also higher than in glendonites (220–600 ppm in glendonites and 1400–1700 ppm in nodules). Similar changes in the concentrations of elements with varying values are noted for Co, Ni, Cu, V, and Cr.

REE (lanthanide + Y) concentrations were normalized for Post-Archean Australian Shale (PAAS, Taylor and McLennan 1985), Ce/Ce\* and Eu/Eu\* anomalies were calculated using equations given in Bau and Dulski (1996), Bau (2006), and Ponnurangam et al. (2016). PAAS-normalized patterns are given in Figure 8. Samples are characterized by weak positive Eu anomaly (1.13–2.29); the Y/Ho ratio varies from 30 to 42. All patterns show similar shape with higher concentration of heavy REE (HREE) and lower concentration in light REE (LREE). PAAS-normalized patterns of host concretions are characterized by a middle REE (MREE) bulge.

#### U/Th dating

All the studied samples contained some amount of  $^{232}\text{Th}$ . A linear regression was constructed for four glendonite subsamples ( $^{230}\text{Th}/^{232}\text{Th} - ^{234}\text{U}/^{232}\text{Th}$  and  $^{234}\text{U}/^{232}\text{Th} - ^{238}\text{U}/^{232}\text{Th}$ , Table 3 and Fig. 10), giving an isochronous age of the carbonate fraction of  $37 \pm 7$  ka.

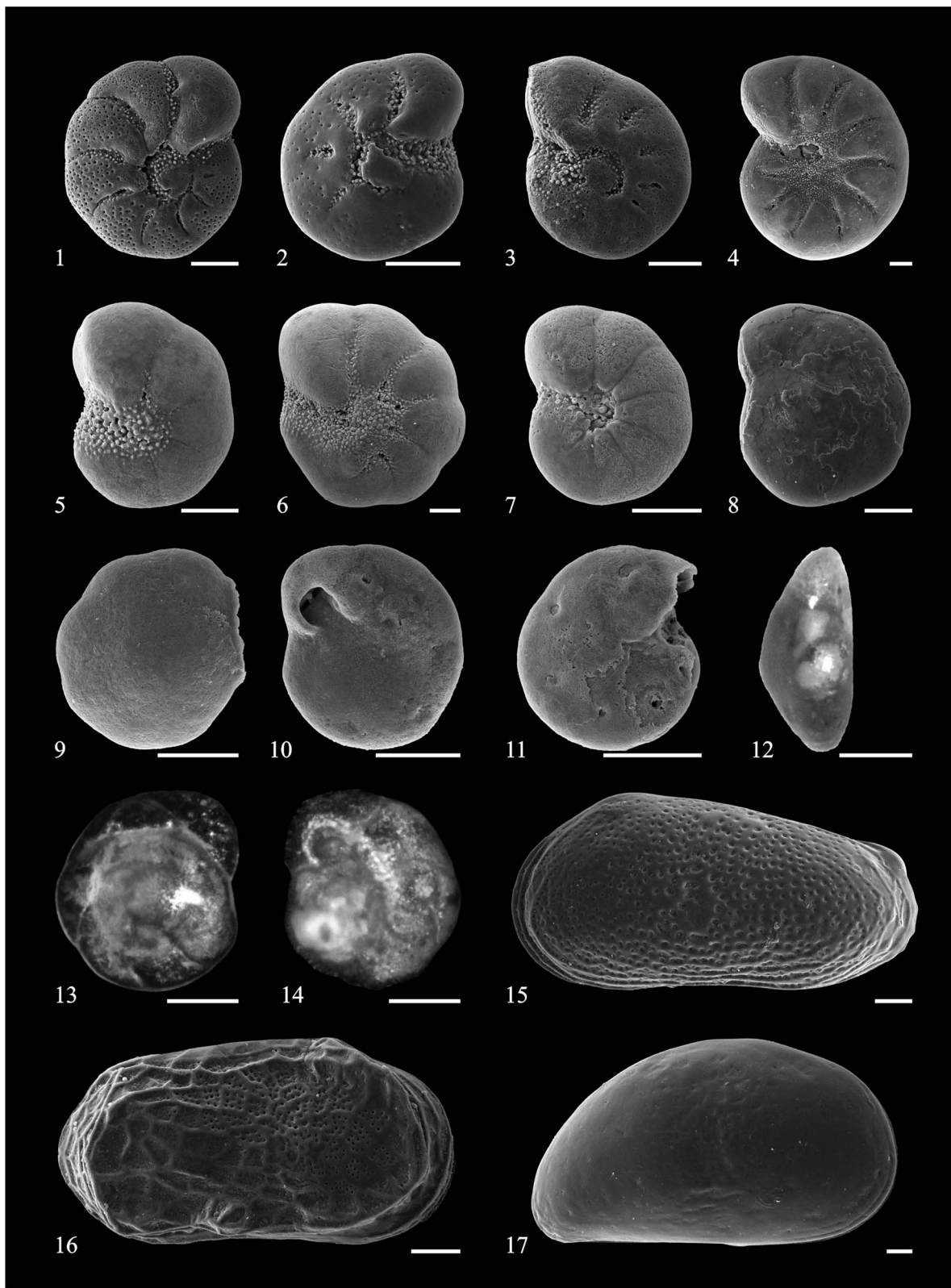


FIG. 4.—Foraminiferal tests and ostracod valves from the Bol'shaya Balakhnya section, eastern part of the Taimyr. Scale bar 50  $\mu\text{m}$ . 1, 12, 15–17, SEM images; 13–15, light microscope images. Foraminifera: 1–3, *Elphidium clavatum* (Cushman 1930); 4, *Elphidium albumbilicatum* (Weiss 1954); 5–7, *Haynesina orbiculare* (Brady 1881); *Buccella frigida* (Cushman 1922); 9–14, *Eoeponidella pulchella* (Parker 1952); 9, 13, dorsal view; 10, 11, 14, ventral view; 12, side view. Ostracods: 15, *Roundstonia macchesneyi* (Brady and Crosskey 1871), left valve external view; 16, *Semicytherura complanata* (Brady et al. 1874), right valve external view; 17, *Sarsicytheridea bradii* (Norman 1864), right valve external view.

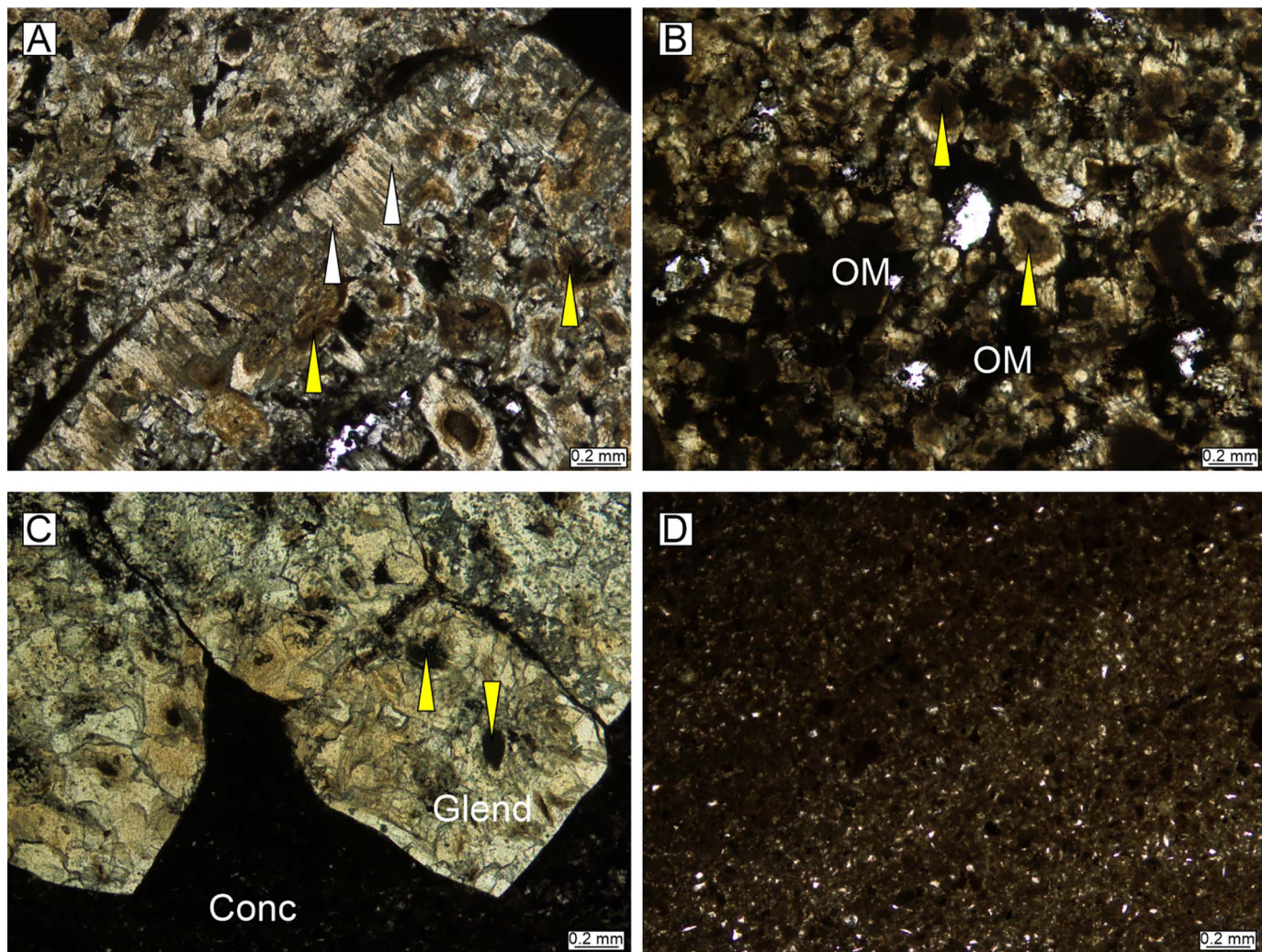


FIG. 5.—Optical characteristics of the studied glendonites and host concretions in plane-polarized light. **A)** Sample Sn-1 (glendonite). **B)** Sample Bal-6 (glendonite). **C)** Sample Bal-2 (Glend, glendonite; Conc, host concretion). **D)** Sample Bal-4 (host concretion). White arrows point at needle-like calcite crystals at the edge of a glendonite blade, yellow arrows point at dark central zones of the glendonite-composing crystals.

## DISCUSSION

### *Age Constraints on Ikaite Crystallization and Transformation*

The stratigraphy of the Quaternary deposits north of the Siberian platform and of the Taimyr Peninsula has been discussed in several reviews (Arslanov et al. 2004; Astakhov 2013; Gusev et al. 2016; Möller et al. 2019, among others). Recent advances in dating techniques applied to Quaternary

TABLE 2.—*Isotope composition of the glendonites and host concretions.*

No.	Sample	$\delta^{13}\text{C}$ , ‰ V-PDB	$\delta^{18}\text{O}$ , ‰ V-PDB
1	Bal-1 (host concretion)	−6.7	−4.2
2	Bal-1 (glendonite)	−8.0	−2.8
3	Bal-2 (glendonite)	−16.0	−2.1
4	Bal-2 (concretion)	−11.0	−2.4
5	Bal-3 (glendonite)	−33.9	−1.1
6	Bal-4 (host concretion)	−22.3	−2.9
7	Bal-4 (glendonite)	−20.3	−1.9
8	Bal-5 (glendonite)	−6.2	−3.5
9	Bal-6 (glendonite)	−23.6	−1.7
10	Sn-1 (glendonite)	−20.0	−2.1

deposits allow measurement of ages using different approaches, but still some uncertainties remain.

Sediments exposed in the terraces of the Bol'shaya Balakhnya River that contain glendonites were described by Kind and Leonov (1982) and Mokhov and Proskurnin (2015). Mokhov and Proskurnin (2015) propose that the marine deposits exposed along the Bol'shaya Balakhnya River correspond to the Kazantsevo Formation, while Kind and Leonov propose that these deposits date back to the later Karginian time (interstadial). According to published stratigraphical schemes for the Taimyr Peninsula, the accumulation of the Kazantsevo Formation was preceded by the Taz glaciation, corresponding to MIS 6 and the Moscow glaciation in the European part of Russia (Volkova and Babushkin 2000). Numerous datings (OSL, ESR, U/Th) for the Kazantsevo Formation from the northern part of Western Siberia and the Taimyr Peninsula reveal ages from ~ 70 to ~ 120 ka (Kind and Leonov 1982; Arkhipov 1989; Gusev et al. 2016; Kostin et al. 2019) corresponding to MIS 5.

Sediments of the Kazantsevo Formation indicate climate warming and inflows of Atlantic water into the Arctic (Astakhov 2013). The Kazantsevo sediments contain the boreal mollusk *Arctica islandica* and the extinct index mollusk *Cyrtodaria jennisseeae* (= *C. angusta* in modern systematics) (Sachs 1953). The presence of thermophilic plants and mollusk remnants provides information on a milder and warmer climate than nowadays (Arslanov

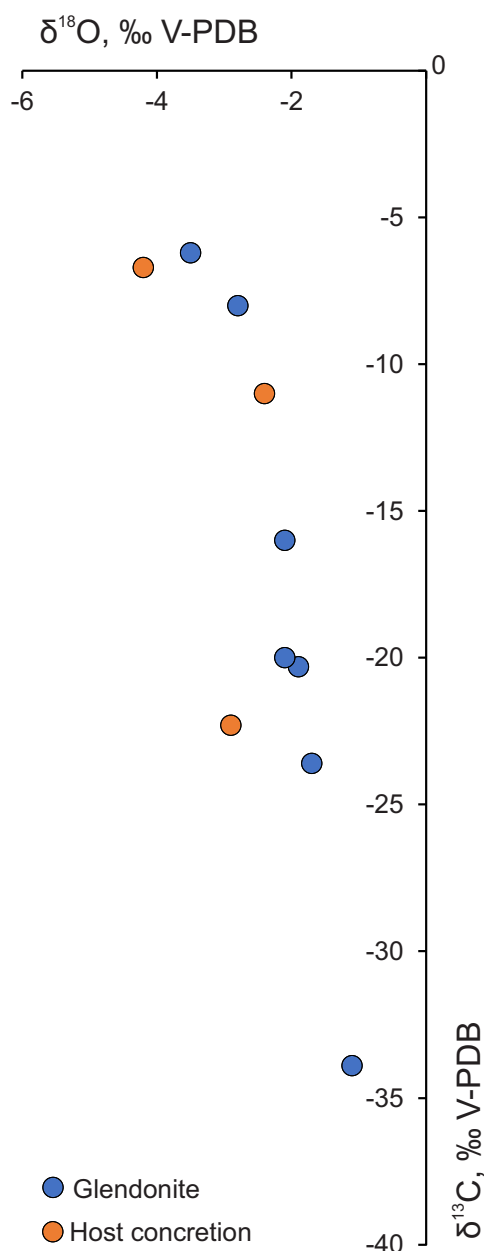


Fig. 6.—Isotope composition of the studied glendonites and host concretions.

et al. 2004; Volkova et al. 2010; Gusev et al. 2016). The area of the modern Taimyr and Yenisey rivers is located in a basin where sands, silts, and coarse gravels were deposited; the sedimentary basin was probably slightly desalinated (Mezhubovskiy et al. 2001). Based on microfaunal complexes from the Kazantsevo deposits of Taimyr, it is shown that the basin was shallow (up to 50 m in depth) (Kind and Leonov 1982).

According to the assumptions of Sachs (1953), the Kazantsevo was followed by the most extensive glaciation of the late Quaternary, the Zyryanka glaciation. The Karginsky interstadial is believed to divide two independent glaciations—the major Early Zyryanka and minor Later Zyryanka. It is supposed (Gudina 1976; Kind and Leonov 1982; Levchuk 1984) that the Karginsky Formation was deposited in an even warmer sea than the Kazantsevo Formation. <sup>14</sup>C dating of plant detritus showed ages between  $46.7 \pm 1.2$  ka to  $26 \pm 1$  ka (Kind and Leonov 1982); Arkhipov (1989) documented a similar age, 22–50 ka (<sup>14</sup>C), for the Karginsky deposits.

Some new information on <sup>14</sup>C ages of foraminifera tests found in the Karginsky Formation in the westernmost part of Taimyr were determined as  $31.31 \pm 0.4$  ka and  $39 \pm 1.11$  ka (Gusskov et al. 2008). Thus, the Karginsky transgression corresponds with MIS 3. Based on the faunal complex, Kind and Leonov (1982) suggest that the Karginsky sea basin was shallow (40–50 m), characterized by slightly reduced salinity and bottom temperatures slightly above zero. The Karginsky deposits are overlain by either later continental sediments (alluvial, lacustrine–alluvial) or glacial ones, corresponding to the Sartan (Upper Zyryanka) glaciation.

Foraminifera determined from the clays with glendonites from the Bol'shaya Balakhnya section belong to species that inhabit modern Arctic and Nordic seas (Polyak et al. 2002; Korsun et al. 2014) and are found in Holocene and Pleistocene marine sediments of northern Eurasia as well (Gudina 1976; Levchuk 1984; Zanina et al. 2021; Taldenkova et al. 2024). *B. frigida*, *E. clavatum*, *E. albumbilicatum*, and *H. orbiculare* belong to the river-proximal ecological group (Polyak et al. 2002). These species with *E. pulchella* were also found in Karginsky section A-47 on the Bol'shaya Balakhnya River, but the foraminiferal assemblages were richer (Levchuk 1984). Ostracods are represented by two shallow-water marine species *S. complanata*, *S. bradii* and a brackish-water species *R. macchesneyi*, which are typical of the modern fauna of the Kara and Laptev Sea shelves (Stepanova et al. 2007). These benthic microfaunal groups are not important for determining the exact age of the host sediments, but they do confirm that sedimentation occurred on a shallow shelf that was influenced by river runoff (details of the ecology of these Foraminifera and Ostracoda species are described in Polyak et al. 2002, Stepanova et al. 2007, and Korsun et al. 2014).

The age obtained by U/Th dating of glendonites is  $37 \pm 7$  ka, and this age largely corresponds to the age of the Karginsky horizon. Currently, there is no data on the fractionation of U and Th isotopes during the dehydration of ikaite and ikaite–glendonite transformation, the assumption being that U/Th dating gives ages that agree with <sup>14</sup>C dating at least within the first thousand years (Vasileva et al. 2022).

Kind and Leonov (1982) mentioned glendonites (as “gennoishe”) specifically from the Karginsky layers of Bol'shaya Balakhnya River middle flows (A-47, A-50, and A-51 sections, southwards from Dolgoe Lake) and indicate that the microfauna diversity in dark-colored clay layers with glendonites decreases. These authors also propose that glendonite occurrence in clay layers indicate the marine origin of the layers. Although ikaite and glendonite can be found in non-marine settings (lakes (Council and Bennett 1993; Last et al. 2013; Oehlerich et al. 2013), caves (Bazarova et al. 2016, 2018), and ice (Brown et al. 2015)), our identification of microfauna in clays enclosing glendonites confirms that studied sediments are of marine origin.

The dark-colored clay of the Karginsky Formation is overlain by Sartan limnoglacial light-colored sands that contain ice wedges and do not contain any faunal remnants (Kind and Leonov 1982). Thus, the section shows a gradual shallowing of the basin and the possible transition of shallow marine clayey sediments to sand deposited in a continental environment. The absence of glendonites in the coarser-grained sands of the Karginsky Formation may be caused by better aeration of the sand and rapid aerobic oxidation of organic matter instead of anaerobic oxidation necessary for sulfate reduction (see below, Isotopic and Geochemical Constraints on Environment of Ikaite Precipitation and Transformation).

In modern environments, ikaite is linked to near-freezing bottom temperature (below 7°C, Domack et al. 2007; Logvina et al. 2018; Tollefsen 2018, among others). The absence of glendonites in the overlying lacustrine sediments of the Sartan glaciation, which bear traces of at least a seasonal temperature below zero for bottom water, suggests that low temperatures are not the only condition for the formation and transformation of ikaite. Probably another important factor controlling ikaite precipitation was the presence of seawater (containing  $\text{SO}_4^{2-}$  for sulfate reduction) combined with the presence of organisms supplying organic matter to the sediments. The simultaneous implementation of these conditions in the sedimentary basin occurred only at the end of

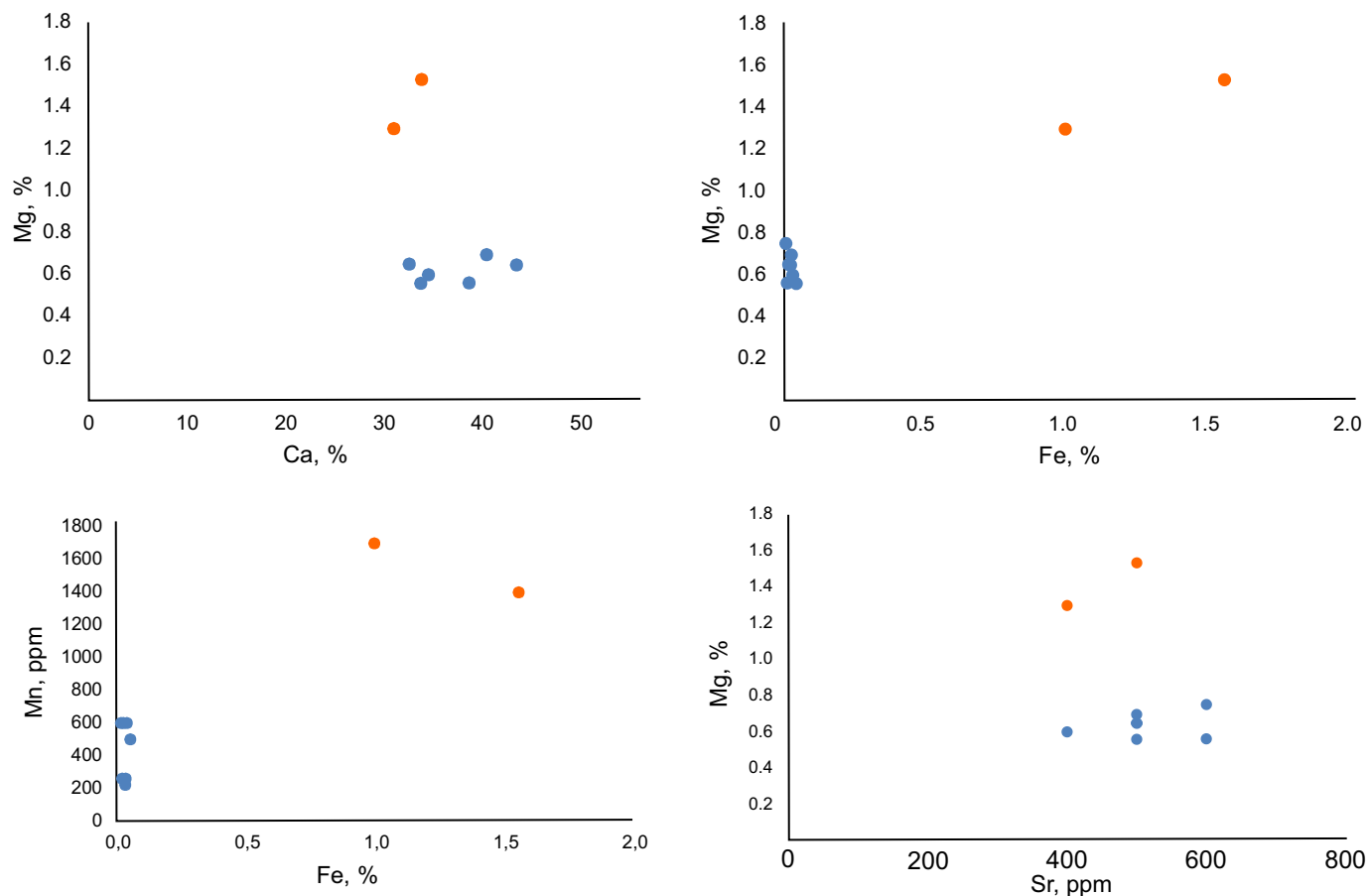


FIG. 7.—Ca-Mg, Fe-Mg, Fe-Mn, Sr-Mg concentration cross-plots. Blue points are for glendonites while orange points are for concretions.

Karginsky time, when: 1) the marine basin still existed, 2) the sediments contained a certain amount of organic matter dispersed in fine clayey silt, and 3) cooling and gradual shallowing of the basin began, which could promote a more contrasting change in bottom temperatures due to seasonal temperature changes.

#### *Isotopic and Geochemical Constraints on Environment of Ikaite Precipitation and Transformation*

Complex mineralogical (morphology, composition) and petrographic features reveal that the studied glendonites of the eastern Taimyr are similar to Holocene glendonites described from the White Sea (northwestern Russia, Schultz et al. 2022; Vasileva et al. 2022). The glendonites are composed of two calcite types—dark tabular calcite crystals or rosette aggregates that are surrounded with acicular needle-like crystals. A certain amount of organic matter is also a constituent of the pseudomorph; organic matter fills pore space between calcite crystals. Concretions around glendonites are composed of high-magnesium calcite (micrite) cementing silt-size quartz grains. Because the concretion includes (overgrowths) the glendonite pseudomorph, we assume that concretion growth occurred later than ikaite precipitation and possibly later than ikaite–glendonite transformation.

Ikaite crystallization and transformation occurred due to decomposition of organic matter causing the isotopic composition of the studied glendonites. The  $\delta^{13}\text{C}$  in the studied samples varies from  $-33.9$  to  $-6.2\%$  V-PDB (mean value  $-18.2\%$  V-PDB), reflecting decomposition of organic matter which promoted ikaite precipitation (Muramiya et al. 2022; Vickers et al. 2022; Counts et al. 2024). It seems that the presence of organic matter played a

crucial role in promoting ikaite crystallization as glendonite pseudomorphs were found only in dark organic-rich clays. The lowest value of  $\delta^{13}\text{C}$  ( $-33.9\%$  V-PDB, sample Bal-3) indicates that some amount of methane could also percolate into the ikaite crystallization zone. Methane could form during biological methanogenesis performed by anaerobic bacteria inhabiting sediments in the zone of methanogenesis (Whiticar 1999); as methane percolates upward through sediments, in the zone of anaerobic methane oxidation or in the zone of sulfate reduction, methane undergoes anaerobic oxidation (Smrzka et al. 2020; Munnecke et al. 2023).

The values of  $\delta^{18}\text{O}$  in glendonites vary from  $-3.5$  to  $-1.1\%$  V-PDB that is very close to isotopic composition of seawater-derived calcite (Campbell 2006); low negative values of  $\delta^{18}\text{O}$  (lower than  $-2\%$  V-PDB) indicate either influence of meteoric fresh water or influence of late diagenetic fluids (Campbell 2006). The glendonites lack true negative Ce/Ce\* anomalies, but the overall shape of PAAS-normalized REE patterns (Fig. 9) is close to seawater with HREE enrichment (e.g., Tostevin et al. 2016) which also confirms the influence of seawater during ikaite precipitation and transformation.

Apparently, carbon for cementation of the surrounding sediments and concretion precipitation was derived from the same sources—decomposition of organic matter and dissolved seawater inorganic carbon (the values of  $\delta^{13}\text{C}$  in concretions vary from  $-22.3$  to  $-6.7\%$  V-PDB; Fig. 6). The concretions are composed of high-magnesium calcite (HMC), and geochemical characteristics of host concretions and glendonite slightly differ. Concretions are characterized by a low Ca/Mg ratio and elevated concentrations of redox-sensitive elements Fe, Mn, Zn, Cd, and U (Fig. 8, Table S1) compared to glendonites. According to Smrzka et al. (2020), enrichment of the redox-sensitive elements depends on the diagenetic environment: Fe- and

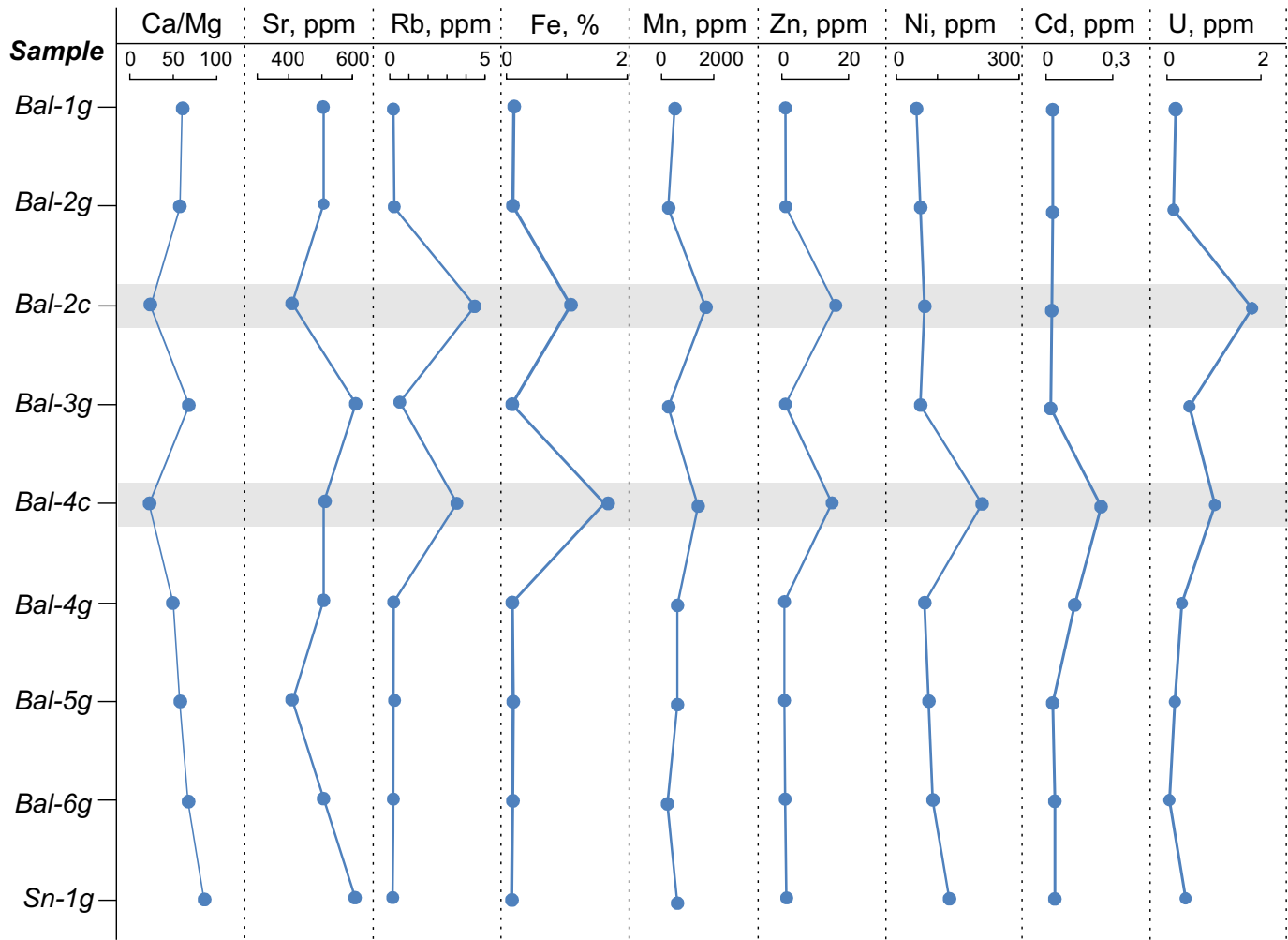


FIG. 8.—Changes in the concentrations of Sr, Rb, Fe, Mn, Zn, Ni, Cd, U, and Ca/Mg ratio in the studied samples of glendonites and host concretions. Gray rectangles mark changes in geochemical composition of host nodules.

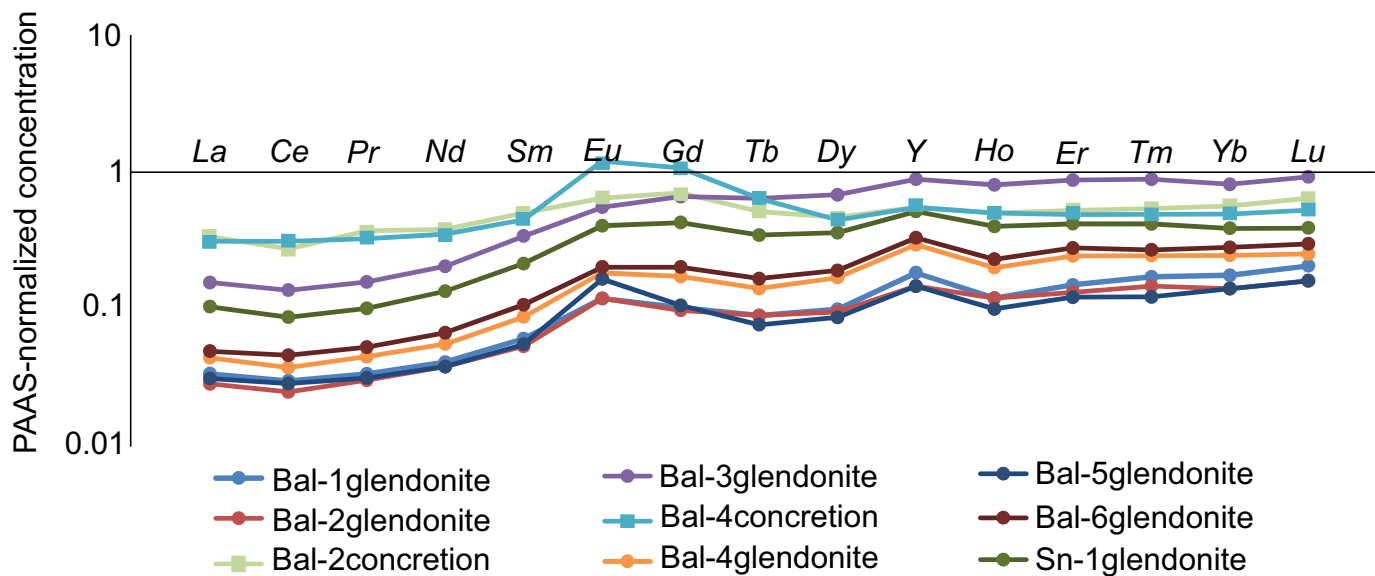


FIG. 9.—Patterns of PAAS-normalized concentrations of REE.

TABLE 3.—Results of the radiochemical analyses of four sub-samples of Bal-4 sample determined applying TSD technique.

No.	$^{238}\text{U}$	$^{234}\text{U}$	$^{230}\text{Th}$	$^{232}\text{Th}$	$^{230}\text{Th}/^{234}\text{U}$	$^{234}\text{U}/^{238}\text{U}$
	dpm/g					
1	$0.333 \pm 0.019$	$0.424 \pm 0.022$	$0.276 \pm 0.013$	$0.103 \pm 0.008$	$0.650 \pm 0.046$	$1.274 \pm 0.093$
2	$0.360 \pm 0.015$	$0.439 \pm 0.016$	$0.340 \pm 0.018$	$0.149 \pm 0.011$	$0.774 \pm 0.050$	$1.219 \pm 0.062$
3	$0.362 \pm 0.027$	$0.520 \pm 0.034$	$0.328 \pm 0.022$	$0.141 \pm 0.014$	$0.630 \pm 0.059$	$1.438 \pm 0.132$
4	$0.500 \pm 0.043$	$0.584 \pm 0.049$	$0.345 \pm 0.018$	$0.126 \pm 0.011$	$0.591 \pm 0.058$	$1.168 \pm 0.130$

dpm/g, decay per minute per gram.

Mn-reduction of organic matter results in U and Cd enrichment, while sulfate reduction results in enrichment of Mo, Co, Cu, Ni, Zn, and V.

The process that affects ikaite precipitation and transformation to glendonite is organoclastic sulfate reduction and Fe–Mn reduction (Qu et al. 2017). Sulfate reduction is a complex biogenic process that involves sulfate reduction to sulfides coupled with anaerobic methane or organic matter oxidation (Machel et al. 2001; Qu et al. 2017, among others). Fe–Mn reduction leads to a Fe(III)–Fe(II) transition and/or a Mn(IV)–Mn(II) transition during the redox reactions (Liu et al. 2022). Both reduction processes result in production of  $\text{CO}_2$  (during oxidation of organic matter and/or methane) and high pH (alkaline environment) promoting authigenic carbonate precipitation. Thus, it is likely that common chemical reactions led to precipitation of different authigenic carbonates (ikaite versus HMC in concretion). Nevertheless, at low temperatures there are some kinetics preventing high-magnesium calcite precipitation (Purgstaller et al. 2017), while low temperatures favor ikaite

precipitation (Hu et al. 2014; Zhou et al. 2015; Purgstaller et al. 2017). The differences in chemical composition of the distinct types of authigenic carbonates can be explained by differences in the crystalline structure of low- and high-magnesium calcite.

Thus, organoclastic sulfate reduction and Fe–Mn reduction are probably the main processes affecting both ikaite and HMC precipitation. However, there can be some factors (e.g., temperature, level of sulfate reduction, presence of specific microbial communities) that require additional research.

#### CONCLUSION

This study represents the first multiproxy study of the Pleistocene glendonites from the outcrops of the Bol'shaya Balakhnya River, northern Taimyr. U–Th dating shows that the glendonites have an age of  $37 \pm 7$  ka, which correlates well with the ages of the Karginsky horizon (MIS 3) of the

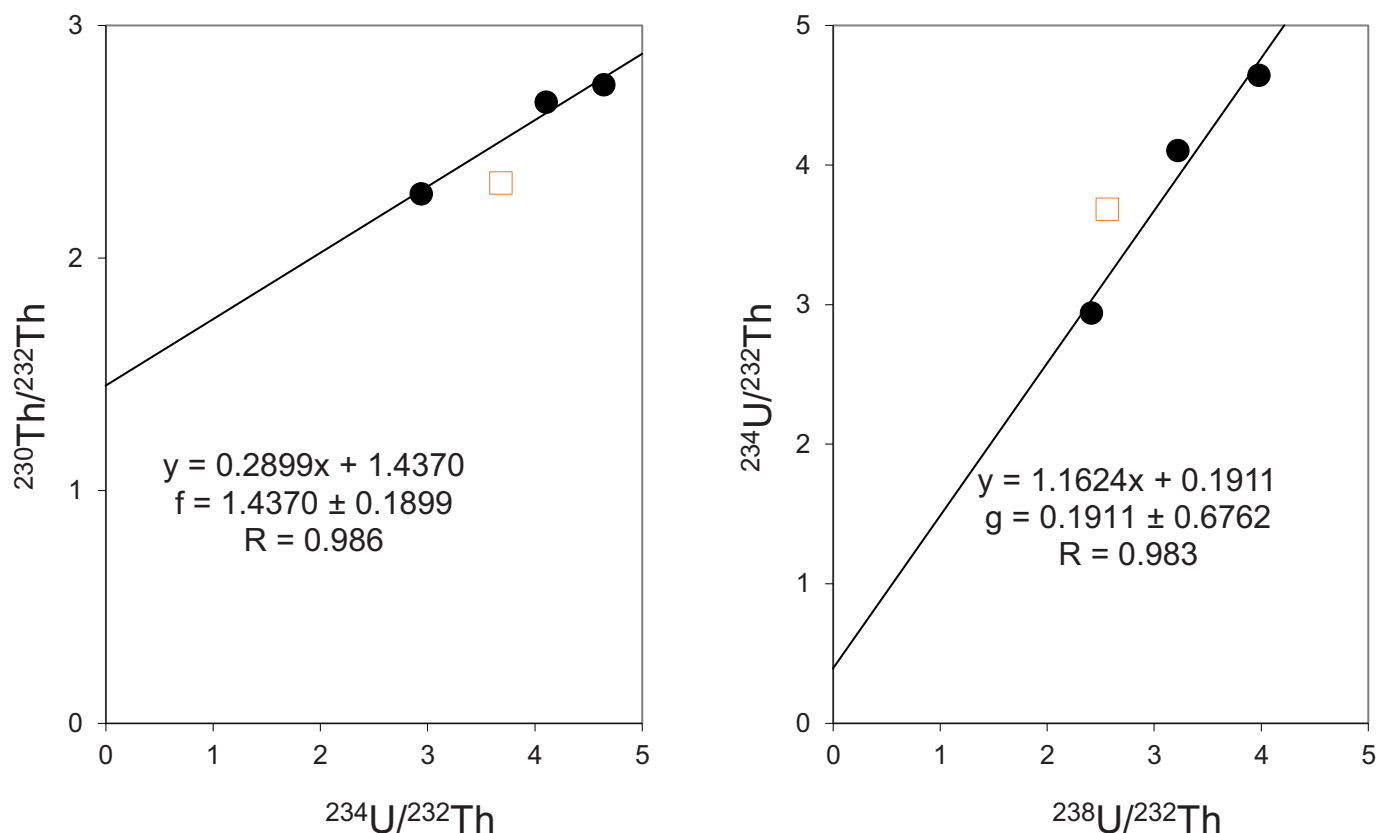


FIG. 10.—Isochron linear relationships showing the activity ratios:  $^{230}\text{Th}/^{232}\text{Th}$  versus  $^{234}\text{U}/^{232}\text{Th}$  (left) and  $^{234}\text{U}/^{232}\text{Th}$  versus  $^{238}\text{U}/^{232}\text{Th}$  (right). The intercept on the y axis in the plots of  $^{230}\text{Th}/^{232}\text{Th}$  vs  $^{234}\text{U}/^{232}\text{Th}$  and  $^{234}\text{U}/^{232}\text{Th}$  vs  $^{238}\text{U}/^{232}\text{Th}$  isotope activity gives the values correction indices f and g required for defining the  $^{230}\text{Th}/^{234}\text{U}$  and  $^{234}\text{U}/^{238}\text{U}$  ratios in the clastic-free carbonate fraction. One subsample (orange square) was excluded from consideration as inconsistent with the linear regression. The isochronous age calculated from these activity ratios is  $37 \pm 7$  ka.

late Pleistocene of Taimyr and have proven the data obtained earlier by other methods ( $^{14}\text{C}$  dating of plant remnants (Kind and Leonov 1982) and foraminifera tests (Gusskov et al. 2008)). Based on reconstructions of climate and environmental changes in the Pleistocene for the Taimyr region, it is supposed that extensive warming during Karginsky time led to transgression and the formation of a wide shallow basin with terrigenous sedimentation, when sands, silts, and clays accumulated. Foraminifera tests (*E. clavatum*, *E. albiumbilicatum*, *B. frigida*, *H. orbiculare*) and ostracod valves (*S. complanata*, *S. bradii*, *R. macchesneyi*) from the studied section confirm that sedimentation occurred in the shallow basin that was highly influenced by inflow of riverine water. In the studied section, glendonites are found in a layer of dark-colored clay in the upper part of the Karginsky Formation. We propose that ikaite crystallization was triggered by two main factors. First, the anaerobic decomposition of organic matter in fine clayey sediments; the anaerobic oxidation provided an alkaline environment necessary for carbonate precipitation. Most likely, decomposition of organic matter in the light sands was aerobic, and this inhibited ikaite precipitation. Second, shallowness of the sedimentary environment could lead to seasonal temperature fluctuations, reaching near-freezing temperatures at least during winter months. Isotope studies indicate that the source of carbon for ikaite crystallization and transformation was decomposing organic matter, dissolved inorganic carbon, and probably anaerobic oxidized methane ( $\delta^{13}\text{C}$  in the studied samples vary from  $-33.9$  to  $-6.2\text{‰}$  V-PDB).  $\delta^{18}\text{O}$  isotope ratios, and PAAS-normalized patterns of REE reveal that ikaite crystallization and transformation was influenced by seawater. After crystallization of ikaite and, possibly, its transformation into glendonite, the area around the pseudomorph was gradually cemented by calcite, leading to the formation of a host concretion. Close ratios of  $\delta^{13}\text{C}$  in host nodules and glendonites shows a similar carbon source, and the main process leading to the crystallization of ikaite and calcite was sulfate reduction coupled with decomposition of organic matter. Nevertheless, the geochemical characteristics (Mg/Ca ratio, concentrations of Fe, Mn, Zn, Cd, and U) differ in host concretions and glendonites. This may reflect differences in the crystalline structure of ikaite and high-magnesium calcite.

#### SUPPLEMENTAL MATERIALS

Supplemental materials are available from the SEPM Data Archive: <https://www.sepm.org/supplemental-materials>.

#### ACKNOWLEDGMENTS

We are very grateful to Associate Editor Dr. Sally Sutton, Corresponding Editor Prof. John B. Southard, and two anonymous reviewers, who significantly improved the quality of this manuscript.

The authors acknowledge the Resource Center of X-ray diffraction studies and “Geo-model” Resource Centre of Saint Petersburg State University for providing instrumental and computational resources. The reequipment and comprehensive development of the “Geoanalitik” shared research facilities of the IGG UB RAS is financially supported by a grant from the Ministry of Science and Higher Education of the Russian Federation for 2021–2023 (Agreement No. 075-15-2021-680). ICP-MS and ICP-AES analyses were performed at the “Geoanalitik” shared research facilities and supported by the IGG UB RAS state assignment No.123011800012-9. This study has been carried out following the plans of the scientific research of the Geological Institute of RAS (for VE, MR, and YO, project no. FMMG-2021-0003). We would also like to thank ostracodologist A. Stepanova for consultation on species identification.

#### REFERENCES

- ARKHIPOV, S.A., 1989, The chronostratigraphic scale of the glacial Pleistocene of the West Siberian North, in Skabichevskaya, N.A., ed., Pleistotsen Sibiri, Stratigrafia i Mezhtsionalnye Korrelatsii: Nauka, Novosibirsk, p. 20–30 [in Russian].
- ARSLANOV, K.A., LAUKHIN, S.A., MAKSIMOV, F.E., KUZNETSOV, V.Y., VELICHKEVICH, F.Y., SAN'KO, A.F., SHILOVA, G.N., AND CHERNOY, S.B., 2004, Bedoba: key section of Kazantsovian horizon in Central Siberia: Doklady Earth Sciences, v. 396, p. 796–799.
- ASTAKHOV, V.I., 2013, Pleistocene glaciations of northern Russia: a modern view: Boreas, v. 42, p. 1–24.
- BAU, M., 2006, Preservation of primary REE patterns without Ce anomaly during dolomitization of Mid-Paleoproterozoic limestone and the potential re-establishment of marine anoxia immediately after the “Great Oxidation Event”: South African Journal of Geology, v. 109, p. 81–86.
- BAU, M., AND DULSKI, P., 1996, Distribution of yttrium and rare-earth elements in the Penge and Kuruman iron formations, Transvaal Supergroup, South Africa: Precambrian Research, v. 79, p. 37–55.
- BAZAROVA, E., KONONOV, A., AND GUTAREVA, O., 2016, Cryogenic mineral formations in the Okhotnichya Cave in the Primorsky Mountain Ridge (western Baikal Region, Russia): Eurospeleo Magazine, v. 3, p. 47–59.
- BAZAROVA, E.P., KADEBSKAYA, O.I., AND TSURIKHIN, E.A., 2018, Cryogenic minerals of the r. Vizhay caves (Northern Urals): Bulletin of Perm University, Geology, v. 17, p. 11–17.
- BISCHOFF, J.L., AND FITZPATRICK, J.A., 1991, U-series dating of impure carbonates: an isochron technique using total-sample dissolution: Geochimica et Cosmochimica Acta, v. 55, p. 543–554.
- BRODSKAYA, N.G., AND RENTGARTEN, N.V., 1975, Organogenic origin of diagenetic aggregates the type “gennoishi”: problems of lithology and geochemistry of sedimentary rocks and ores: Moscow, Nauka, p. 312–322.
- BROWN, K.A., MILLER, L.A., MUNDY, C.J., PAPA KYRIAKOU, T., FRANCOIS, R., GOSSELIN, M., CARNAT, G., SWYSTUN, K., AND TORTELL, P.D., 2015, Inorganic carbon system dynamics in landfast Arctic sea ice during the early-melt period: Journal of Geophysical Research, Oceans, v. 120, p. 3542–3566.
- CAMPBELL, K.A., 2006, Hydrocarbon seep and hydrothermal vent paleoenvironments and paleontology: past developments and future research directions: Palaeogeography, Palaeoclimatology, Palaeoecology, v. 232, p. 362–407.
- COUNCIL, T.C., AND BENNETT, P.C., 1993, Geochemistry of ikaite formation at Mono Lake, California: implications for the origin of tufa mounds: Geology, v. 21, p. 971–974.
- COUNTS, J.W., VICKERS, M.L., STOKES, R., SPIVEY, W., GARDNER, K.F., SELF-TRAIL, J.M., GOOLEY, J.T., MCALLEER, R.J., JUBB, A.M., HOUSEKNECHT, D.W., LEASE, R.O., GRIFFIS, N.P., VICKERS, M., SLIWINSKA, K., TOMPKINS, H.G.D., AND HUDSON, A.M., 2024, Insights into glendonite formation from the upper Oligocene Sagavanirktok Formation, North Slope, Alaska, U.S.A.: Journal of Sedimentary Research, v. 94, p. 179–206.
- DELVENTHAL, E., 2022, A selection of glendonites from worldwide localities: a pictorial: Rocks & Minerals, v. 97, p. 510–513.
- DOMACK, E.W., HALVERSON, G., WILLMOTT, V., LEVENTER, A., BRACHFELD, S., AND ISHMAN, S., 2007, Spatial and temporal distribution of ikaite crystals in Antarctic glacial marine sediments: U.S. Geological Survey, Open-File Report 2007-1047, Extended Abstract 015, 5 p.
- GREINERT, J., AND DERKACHEV, A., 2004, Glendonites and methane-derived Mg-calcites in the Sea of Okhotsk, Eastern Siberia: implications of a venting-related ikaite–glendonite formation: Marine Geology, v. 204, p. 129–144.
- GUSEV, E.A., MOLODKOV, A.N., STRELETSKAYA, I.D., VASILIEV, A.A., ANIKINA, N.Y., BONDARENKO, S.A., DEREVYANKO, L.G., KUPRIYANOVA, N.V., MAKSIMOV, F.E., POLYAKOVA, E.I., PUSHINA, Z.V., STEPANOVA, G.V., AND OBLGOV, G.E., 2016, Deposits of the Kazantsevo Transgression (MIS 5) in the northern Yenisei Region: Russian Geology and Geophysics, v. 57, p. 586–596.
- FISHER, E.A., 1989, Report on the production of aerial photogeological mapping and the search for mineral deposits (Yenisei–Khatanga trough): PGO “Aerogeology,” VSEGEI (Russian Geological Research Institute) Foundations [in Russian].
- FRANK, T.D., THOMAS, S.G., AND FIELDING, C.R., 2008, On using carbon and oxygen isotope data from glendonites as paleoenvironmental proxies: a case study from the Permian System of eastern Australia: Journal of Sedimentary Research, v. 78, p. 713–723.
- GEYH, M., 2008, Selection of suitable data sets improves 230 Th/U dates of dirty material: Geochronometria, v. 30, p. 69–77.
- GUDINA, V.I., 1976, Foraminifers, stratigraphy and palaeozoogeography of the marine Pleistocene in the northern USSR: Novosibirsk, Nauka [in Russian].
- GUSSKOV, S.A., KUZMIN, Y.V., LEVCHUK, L.K., AND BURR, J.S., 2008, The first radiocarbon dates on foraminifera shells from the Karginian marine sediments of the Taimyr Peninsula (northern central Siberia) and their interpretation: Doklady Earth Sciences, v. 421, p. 902–904.
- HU, Y.-B., WOLF-GLADROW, D.A., DIECKMANN, G.S., VÖLKER, C., AND NEHRKE, G., 2014, A laboratory study of ikaite ( $\text{CaCO}_3 \cdot 6\text{H}_2\text{O}$ ) precipitation as a function of pH, salinity, temperature and phosphate concentration: Marine Chemistry, v. 162, p. 10–18.
- JACOBSON, M.I., 2014, Glendonite from the Arctic wildlife refuge, North Slope, Alaska: Mineral News, v. 30, p. 15.
- KIND, N.V., AND LEONOV, B.N., 1982, The Antropogene of the Taimyr peninsula: Moscow, Nauka.
- KORSUN, S., HALD, M., GOLIKOVA, E., YUDINA, A., KUZNETSOV, I., MIKHAILOV, D., AND KNYAZEVA, O., 2014, Intertidal foraminiferal fauna and the distribution of Elphidiidae at Chupa Inlet, western White Sea: Marine Biology Research, v. 10, p. 153–166.
- KOSTIN, D.N., ANTONOV, O.M., SCHNEIDER, G.V., AND KRYLOV, A.V., 2019, Quaternary deposits of the Northern Taimyr: new data after geological mapping studies during 2017–2018 (GGS-200 Lenivenskaya area S-45-XI, XII): Relief and Quaternary Formations of Arctic, Subarctic and North-East of Russia, v. 5, p. 27–30.
- KRYLOV, A.A., LOGVINA, E.A., MATVEEVA, T.M., PRASOLOV, E.M., SAPEGA, V.F., DEMIDOVA, A.L., AND RADCHENKO, M.S., 2015, Ikaite ( $\text{CaCO}_3 \cdot 6\text{H}_2\text{O}$ ) in bottom sediments of the

- Laptev Sea and the role of anaerobic methane oxidation in this mineral-forming process: Zapiski RMO, no. 4, p. 61–75.
- LAST, F.M., LAST, W.M., FAYEK, M., AND HALDEN, N.M., 2013, Occurrence and significance of a cold-water carbonate pseudomorph in microbialites from a saline lake: Journal of Paleolimnology, v. 50, p. 505–517.
- LEVCHUK, L.K., 1984, Biostratigraphy of the upper Pleistocene of the Siberian north by foraminifers: Novosibirsk, Nauka [in Russian].
- LIU, J., CHEN, Q., YANG, Y., WEI, H., LAIPAN, M., ZHU, R., HE, H., AND HOCELLA, M.F., 2022, Coupled redox cycling of Fe and Mn in the environment: the complex interplay of solution species with Fe- and Mn-(oxyhydr)oxide crystallization and transformation: Earth-Science Reviews, v. 232, 104105.
- LOGVINA, E., KRYLOV, A., TALDENKOVA, E., BLINOVA, V., SAPEGA, V., NOVIKHIN, A., KASSENS, H., AND BAUCH, H.A., 2018, Mechanisms of late Pleistocene authigenic Fe-Mn-carbonate formation at the Laptev Sea continental slope (Siberian Arctic): Arctos, v. 4, p. 1–13.
- MACHEL, H.G., Bacterial and thermochemical sulfate reduction in diagenetic settings: old and new insights: Sedimentary Geology, v. 140, p. 143–175.
- MAKSIMOV, F., AND KUZNETSOV, V., 2010, The new version of the <sup>230</sup>Th/U-dating method of upper and middle Pleistocene buried organogenic sediments: Saint-Petersburg University Vestnik, Series 7, v.4, p. 94–107 [in Russian].
- MEZHUBOVSKY, V.V., ONICHSHENKO, A.N., AND MAKAROV, S.V., 2001, Report on geological survey and additional geological study on a scale of 1:200,000 in the Shrenkovskaya area of Mountain Taimyr within sheets S-47-VII–XII and S-47-XV, XVI: Report of PA “Norilskgeology.”
- MOKHOV, V.V., AND PROSKURNIN, V.F., 2015, State geological map of the Russian Federation, scale 1:1,000,000, 3rd generation, List S-47 Taymyr-Severozemelskaya series: Saint Petersburg, Kartographicheskaya fabrika VSEGEI (Russian Geological Research Institute).
- MÖLLER, P., BENEDIKTSSON, I.O., ANJAR, J., BENNIKE, O., BERNHARDSON, M., FUNDER, S., HAKANSSON, L.M., LEMDAHL, G., LICCIARDI, J.M., MURRAY, A.S., AND SEIDENKRANTZ, M.-S., 2019, Glacial history and palaeoenvironmental change of southern Taimyr Peninsula, Arctic Russia, during the middle and late Pleistocene: Earth-Science Reviews, v. 196, no. 102832.
- MORALES, C., ROGOV, M., WIERZBOWSKI, H., ERSHOVA, V., SUAN, G., ADATTE, T., FÖLLMI, K.B., TEGELAAR, E., REICHT, G.-J., DE LANGE, G.J., MIDDELBURG, J.J., AND VAN DE SCHOOTBRUGGE, B., 2017, Glendonites track methane seepage in Mesozoic polar seas: Geology, v. 45, p. 503–506.
- MUNNECKE, A., WRIGHT, V.P., AND NOHL, T., 2023, The origins and transformation of carbonate mud during early marine burial diagenesis and the fate of aragonite: a stratigraphic sedimentological perspective: Earth-Science Reviews, v. 239, no. 104366.
- MURAMIYA, Y., YOSHIDA, H., MINAMI, M., MIKAMI, T., KOBAYASHI, T., SEKUCHI, T., AND KATSUTA, N., 2022, Glendonite concretion formation due to dead organism decomposition: Sedimentary Geology, v. 429, 106075.
- OEHLERICH, M., MAYR, C., GRISSHABER, E., LÜCKE, A., OECKLER, O.M., OHLENDORF, C., SCHMAHL, W.W., AND ZOLITSCHKA, B., 2013, Ikaite precipitation in a lacustrine environment: implications for palaeoclimatic studies using carbonates from Laguna Potrok Aike (Patagonia, Argentina): Quaternary Science Reviews, v. 71, p. 46–53.
- POLYAK, L., KORSUN, S., FEBO, L., STANOVY, V., KHUSID, T., HALD, M., PAULSEN, B.E., AND LUBINSKI, D.A., 2002, Benthic foraminiferal assemblages from the southern Kara Sea, a river influenced Arctic marine environment: Journal of Foraminiferal Research, v. 32, p. 252–273.
- PONNURANGAM, A., BAU, M., BRENNER, M., AND KOSCHINSKY, A., 2016, Mussel shells of *Mytilus edulis* as bioarchives of the distribution of rare earth elements and yttrium in seawater and the potential impact of pH and temperature on their partitioning behavior: Biogeosciences, v. 13, p. 751–760.
- PURGSTALLER, B., DIETZEL, M., BALDERMANN, A., AND MAVROMATIS, V., 2017, Control of temperature and aqueous Mg<sup>2+</sup>/Ca<sup>2+</sup> ratio on the (trans-)formation of ikaite: Geochimica et Cosmochimica Acta, v. 217, p. 128–143.
- QU, Y., TEICHERT, B.M.A., BIRGEL, D., GOEDERT, J.L., AND PECKMANN, J., 2017, The prominent role of bacterial sulfate reduction in the formation of glendonite: a case study from Paleogene marine strata of western Washington State: Facies, v. 63, 16 p.
- ROGOV, M., ERSHOVA, V., VERESHCHAGIN, O., VASILEVA, K., MIKHAILOVA, K., AND KRYLOV, A., 2021, Database of global glendonite and ikaite records throughout the Phanerozoic: Earth System Science Data, v. 13, p. 343–356.
- ROGOV, M., ERSHOVA, V., GAINA, C., VERESHCHAGIN, O., VASILEVA, K., MIKHAILOVA, K., AND KRYLOV, A., 2023, Glendonites throughout the Phanerozoic: Earth-Science Reviews, v. 241, no. 104430.
- ROWE, P.J., AND MAHER, B.A., 2000, “Cold” stage formation of calcrete nodules in the Chinese Loess Plateau: evidence from U-series dating and stable isotope analysis: Palaeogeography, Palaeoclimatology, Palaeoecology, v. 157, p. 109–125.
- SACHS, V.N., 1953, The Quaternary Period in the Soviet Arctic: Leningrad, Institute of Geology of the Arctic [in Russian].
- SCHULTZ, B., HUGGETT, J.M., KENNEDY, G.L., BURGER, P., FRIIS, H., JENSEN, A.M., KANSTRUP, M., BERNASCONI, S.M., THIBAUT, N., ULLMANN, C.V., AND VICKERS, M.L., 2022, Petrography and geochemical analysis of Arctic ikaite 16 pseudomorphs from Utqiagvik (Barrow), Alaska: Norwegian Journal of Geology, v. 103, no. 202303.
- SMRZKA, D., FENG, D., HIMMLER, T., ZWICKERA, J., HUB, Y., MONIEND, P., TRIBOVILLARDE, N., CHEN, D., AND PECKMANN, J., 2020, Trace elements in methane-seep carbonates: potentials, limitations, and perspectives: Earth-Science Reviews, v. 208, no. 103263.
- STEPANOVA, A., TALDENKOVA, E., SIMSTICH, J., AND BAUCH, H.A., 2007, Comparison study of the modern ostracod associations in the Kara and Laptev seas: ecological aspects: Marine Micropaleontology, v. 63, p. 111–142.
- TAYLOR, S.R., AND MCLENNAN, S.M., 1985, The Continental Crust: Its Composition and Evolution: Palo Alto, Blackwell Scientific Publications, 312 p.
- TALDENKOVA, E., OVSEPYAN, Y., RUDENKO, O., STEPANOVA, A., AND BAUCH, H.A., 2024, Boreal (Eemian) transgression in the northeastern White Sea Region: multiproxy evidence from Bychye-2 Section: Quaternary, v. 7.
- TEICHERT, B.M.A., AND LUPPOLD, F.W., 2013, Glendonites from an Early Jurassic methane seep: climate or methane indicators?: Palaeogeography, Palaeoclimatology, Palaeoecology, v. 390, p. 81–93.
- TOLLEFSEN, E., STOCKMANN, G., SKELTON, A., MÖRTH, C.-M., DUPRAZ, C., AND STURKELL, E., 2018, Chemical controls on ikaite formation: Mineralogical Magazine, v. 82, p. 1119–1129.
- TOSTEVIN, R., SHIELDS, G.A., TARBUCK, G.M., HE, T., CLARKSON, M.O., AND WOOD, R.A., 2016, Effective use of cerium anomalies as a redox proxy in carbonate-dominated marine settings: Chemical Geology, v. 438, p. 146–162.
- VASILEVA, K., ZARETSKAYA, N., ERSHOVA, V., ROGOV, M., STOCKLI, L.D., STOCKLI, D., KHAITOV, V., MAXIMOV, F., CHERNYSHOVA, I., SOLOSHENKO, N., FRISHMAN, N., PANIKOROVSKY, T., AND VERESHCHAGIN, O., 2022, New model for seasonal ikaite precipitation: evidence from White Sea glendonites: Marine Geology, v. 449, no. 106820.
- VICKERS, M., WATKINSON, M., PRICE, G.D., AND JERRETT, R., 2018, An improved model for the ikaite-glendonite transformation: evidence from the Lower Cretaceous of Spitsbergen, Svalbard: Norwegian Journal of Geology, v. 98, p. 1–15.
- VICKERS, M.L., VICKERS, M., RICKABY, R.E.M., WU, H., BERNASCONI, S.M., ULLMANN, C.V., BOHRMANN, G., SPIELHAGEN, R.F., KASSENS, H., PAGH SCHULTZ, B., ALWMARK, C., THIBAUT, N., AND KORTE, C., 2022, The ikaite to calcite transformation: implications for palaeoclimate studies: Geochimica et Cosmochimica Acta, v. 334, p. 201–216.
- VICKERS, M.L., JONES, M.T., LONGMAN, J., EVANS, D., ULLMANN, C.V., STOKKE, E.W., VICKERS, M., FRIELING, J., HARPER, D.T., CLEMENTI, V.J., AND THE IODP EXPEDITION 396 SCIENTISTS, 2023, Paleocene–Eocene age glendonites from the Norwegian margin: indicators of cold snaps in the hothouse?: European Geosciences Union, EGU sphere, doi:10.5194/cp-20-1-2024.
- VOLKOVA, V.S., AND BABUSHKIN, A.Y., 2000, The Unified Regional Stratigraphic Scheme of the Quaternary of the West Siberian Plain: Explanatory Note: Novosibirsk, Siberian Research Institute of Geology, Geophysics, and Mineral Raw Materials, 64 p. [in Russian].
- VOLKOVA, V.S., BORISOVA, B.A., AND KAMALETINOVA, V.A., 2010, The Unified Regional Stratigraphic Scheme of the Quaternary of the Middle Siberia (Taimyr, Siberian Platform): Explanatory Note: Novosibirsk, Siberian Research Institute of Geology, Geophysics, and Mineral Raw Materials [in Russian].
- WHITICAR, M.J., 1999, Carbon and hydrogen isotope systematics of bacterial formation and oxidation of methane: Chemical Geology, v. 161, p. 291–314.
- WHITICAR, M.J., AND SUESS, E., 1998, The cold carbonate connection between Mono Lake, California and the Bransfield Strait, Antarctica: Aquatic Geochemistry, v. 4, p. 429–454.
- WHITICAR, M.J., SUESS, E., WEFER, G., AND MÜLLER, P.J., 2022, Calcium carbonate hexahydrate (ikaite): history of mineral formation as recorded by stable isotopes: Minerals, v. 12, no. 1627.
- ZANINA, O.G., LOPATINA, D.A., OVSEPYAN, Y.S., KUZ'MINA, S.A., STEPANOVA, A.Y., TALDENKOVA, E.E., VISHNIVITSKAYA, T.A., AND RIVKINA, E.M., 2021, Environmental evolution of Cape Maly Chukochy (Kolyma Lowland) in the middle–late Neopleistocene: micropaleontological evidence: Stratigraphy and Geological Correlation, v. 29, p. 722–741.
- ZHOU, X., LU, Z., RICKABY, R.E.M., DOMACK, E.W., WELLNER, J.S., AND KENNEDY, H.A., 2015, Ikaite abundance controlled by porewater phosphorus level: potential links to dust and productivity: The Journal of Geology, v. 123, p. 269–281.

Received 22 December 2023; accepted 23 April 2024.